

Searches for Higgs boson pair production with ATLAS

ARNAUD FERRARI, ON BEHALF OF THE ATLAS COLLABORATION

*Department of Physics and Astronomy
Uppsala University, SE-75120 Uppsala, SWEDEN*

The search for Higgs boson pair (HH) production is at the core of the ATLAS experimental program, as it probes the Brout-Englert-Higgs mechanism, as well as new physics beyond the Standard Model. Based on the proton-proton collision data recorded by the ATLAS experiment at CERN's Large Hadron Collider in 2015 and 2016, three public results on the search for $HH \rightarrow bbbb$, $HH \rightarrow bb\gamma\gamma$ and $HH \rightarrow WW\gamma\gamma$ were recently released and are summarised in these proceedings.

PRESENTED AT

Thirteenth Conference on the Intersections of
Particle and Nuclear Physics (CIPANP 2018)

Indian Wells, California, USA, May 29 to June 3, 2018

1 Introduction

The discovery of the Higgs boson (H) by the ATLAS and CMS Collaborations at the Large Hadron Collider (LHC) in 2012 [1, 2] has confirmed the Brout-Englert-Higgs (BEH) mechanism of electroweak symmetry breaking and mass generation [3, 4]. The Higgs boson mass is about 125 GeV [5] and its measured properties are in agreement with the Standard Model (SM) predictions [6]. However, the BEH mechanism does not only predict the existence of a massive scalar particle, but it also requires the Higgs boson to couple to itself. In order to measure the Higgs potential and thereby have a complete description of the SM, it is necessary to observe the production of Higgs boson pairs and measure the Higgs self-coupling λ_{HHH} . Also, any deviation from the SM predictions would open a window on new physics.

In the SM, Higgs boson pairs (HH) can be produced either in a heavy-quark loop or via Higgs self-coupling, see the left-hand and central diagrams of Figure 1, respectively. However, due to the destructive interference between the two diagrams, the SM Higgs boson pair production is only 33.41 fb at 13 TeV, as computed at the next-to-leading-order (NLO) in QCD and fully accounting for top-quark mass effects [7, 8]. Still, the HH cross-section can be significantly enhanced in several Beyond-the-Standard-Model (BSM) scenarios, e.g. through anomalous couplings, new contact interactions, or resonant production of HH pairs, as illustrated in the right-hand diagram of Figure 1. Several BSM theories indeed predict the existence of heavy particles decaying into a pair of Higgs bosons. For instance, two-Higgs-doublet models (2HDMs) [9, 10] have a second CP-even Higgs boson, which may be heavy enough to decay into two SM-like lighter Higgs bosons. Alternatively, HH pairs can be produced in the decay of a spin-2 graviton, as predicted in the Randall-Sundrum model of warped extra dimensions [11].

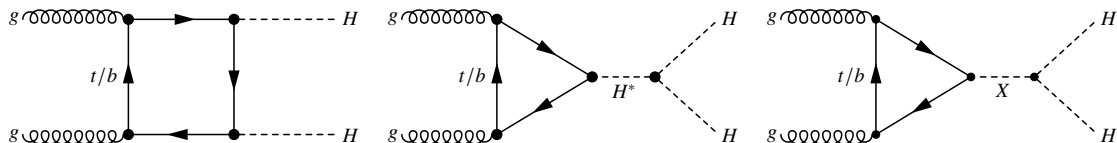


Figure 1: Leading-order Feynman diagrams for HH production in the gluon-gluon fusion mode, via (left) a heavy-quark loop and (centre) Higgs self-coupling in the SM, or through (right) an intermediate resonance (X).

Searches for non-resonant and resonant HH production were conducted by the ATLAS collaboration, based on proton-proton (pp) collision data corresponding to an integrated luminosity of up to 36.1 fb^{-1} . The ATLAS experiment [12–14] is a multi-purpose detector with a forward-backward symmetric cylindrical geometry and nearly

4π coverage in solid angle.* It consists of an inner tracking detector surrounded by a thin superconducting solenoid providing a 2 T axial magnetic field, electromagnetic and hadron calorimeters, and a muon spectrometer. A two-level trigger [15,16] reduces the event rate to a maximum of 1 kHz prior to offline data storage. Three search results were recently published by the ATLAS Collaboration, in the $HH \rightarrow bbbb$ [17], $HH \rightarrow bb\gamma\gamma$ [18] and $HH \rightarrow WW\gamma\gamma$ [19] channels. They are summarised in the following sections of these proceedings.

2 Search for $HH \rightarrow bbbb$ in ATLAS

With a branching fraction of 33%, $HH \rightarrow bbbb$ has the largest event rate among all Higgs boson pair production channels. However, it also suffers from a large multi-jet background, which requires the use of novel data-driven estimation techniques. Depending on the HH production mode and the probed mass range, two event topologies are considered:

- For both the non-resonant HH production mode and the search for a resonance decaying via $HH \rightarrow bbbb$ with a mass in the range 260–1400 GeV, a resolved topology is considered, where at least four anti- k_T jets [20] with a parameter radius $R = 0.4$ are reconstructed with a transverse momentum $p_T > 40$ GeV, and the number of b -tagged jets (i.e. jets compatible with a b -hadron decay) is required to be exactly four (the efficiency of the working point is 70% in simulated $t\bar{t}$ events). Such events are recorded based on a combination of b -tagged jet triggers. Due to an inefficiency of vertex reconstruction and thereby b -tagging at the trigger level, a fraction of the data collected in 2016 was not retained, hence the integrated luminosity for this event topology is only 27.5 fb^{-1} .
- For the search for a resonance decaying via $HH \rightarrow bbbb$ with a mass in the range 800–3000 GeV, a boosted topology is considered, where at least two anti- k_T jets with a larger parameter radius $R = 1.0$ are reconstructed (including one firing the corresponding trigger). The leading (sub-leading) large- R jet is required to have $p_T > 450$ (250) GeV. Then, b -tagging is performed on track-jets with a parameter radius $R = 0.2$ and at least one b -tag per large- R jet is required, which yields three event categories with two, three or four b -tags.

*ATLAS uses a right-handed coordinate system with its origin at the nominal interaction point (IP) in the centre of the detector and the z -axis along the beam pipe. The x -axis points from the IP to the centre of the LHC ring, and the y -axis points upwards. Cylindrical coordinates (r, ϕ) are used in the transverse plane, ϕ being the azimuthal angle around the z -axis. The pseudo-rapidity is defined in terms of the polar angle θ as $\eta = -\ln \tan(\theta/2)$, and the angular distance is measured in units of $\Delta R \equiv \sqrt{(\Delta\eta)^2 + (\Delta\phi)^2}$.

2.1 Resolved topology

For events with a resolved topology, the four jets with highest b -tagging scores are used. The selection and pairing of jets into Higgs boson candidates is performed using angular distances between jets (ΔR_{jj}), the four-jet invariant mass m_{4j} and differences in m_{2j} . Then, m_{4j} - and m_{2j} -dependent requirements on the p_T and mass of the Higgs boson candidates are applied. Events in which a three-jet combination is compatible with a top-quark decay are vetoed to reduce the $t\bar{t}$ background contamination. As a result, the signal region is defined by a small area in the $(m_{2j}^{\text{lead}}; m_{2j}^{\text{sub-lead}})$ phase-space centered at (120 GeV; 110 GeV), corresponding to the reconstructed masses of the two (leading and sub-leading) $H \rightarrow bb$ candidates, as illustrated by the red dashed line in the left-hand plot of Figure 2. The efficiency of the various event selections is shown in the central (right-hand) plot of Figure 2 for various masses of a spin-0 resonance decaying to a Higgs boson pair (non-resonant HH production).

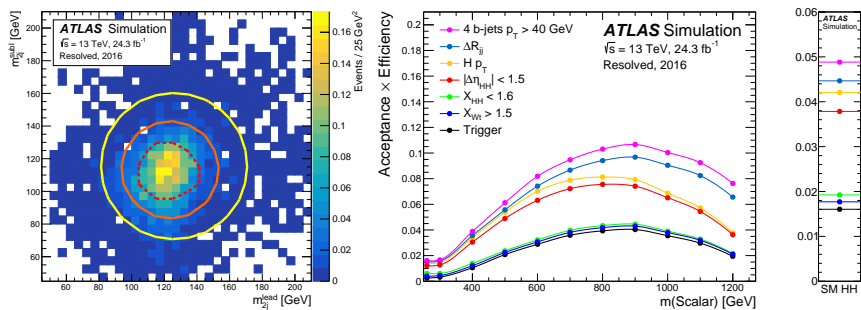


Figure 2: Analysis regions in the $(m_{2j}^{\text{lead}}; m_{2j}^{\text{sub-lead}})$ phase-space (left) where the area within the red dashed line is the signal region, while the area between the orange and yellow full lines is the sideband region used for data-driven background estimation, and event selection efficiencies for a spin-0 resonance decaying to a Higgs boson pair (centre) and non-resonant HH production (right) [17].

The dominant multi-jet background is estimated with data. A data sample is built with the nominal event selection, but the number of b -jets is requested to be exactly two: one H candidate is reconstructed from the two b -tagged jets, and the other one from two non- b -tagged jets. Re-weighting is then applied to this $2b+2j$ sample. The weights are derived by comparing $2b+2j$ and $4b$ samples in a sideband region, located between the orange and yellow full lines in the $(m_{2j}^{\text{lead}}; m_{2j}^{\text{sub-lead}})$ phase-space: a per-non- b -tagged-jet factor is obtained by comparing jet multiplicities and a global event weight is obtained from the ratio of $4b$ and $2b+2j$ templates (after subtracting $t\bar{t}$ events) for five variables sensitive to differences in b -tagging. As for the $t\bar{t}$ background, its shape is taken from simulation, but the normalisations of the fully-hadronic and semi-leptonic $t\bar{t}$ backgrounds are determined together with the multi-jet event yield by a simultaneous fit in three background-enriched regions of the sideband region. A

validation of the background estimate is performed in a dedicated region, which is between the orange full line and the red dashed line in the left-hand plot of Figure 2, and a good agreement between the predicted and measured m_{4j} distribution is found.

Figure 3 shows the invariant mass distribution the two Higgs boson candidates in the signal region, split between the 2015 and 2016 datasets, as different trigger configurations were used. The largest local deviation has a statistical significance of 3.6σ at 280 GeV, while the global significance is 2.3σ .

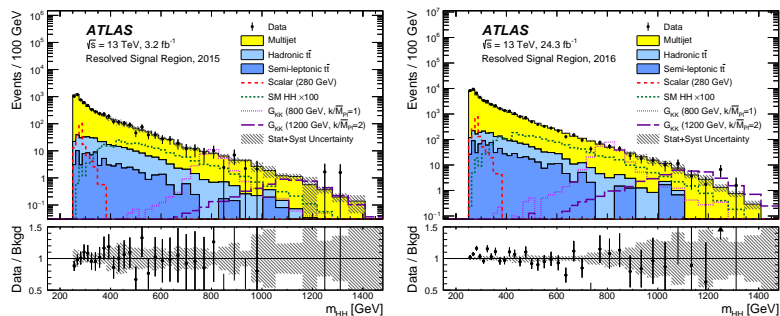


Figure 3: Reconstructed invariant mass of the two $H \rightarrow bb$ candidates in the signal region of the resolved topology, split by data-taking year [17].

2.2 Boosted topology

In the boosted topology, the two large- R jets with highest p_T are used in order to reconstruct the two $H \rightarrow bb$ candidates, with an angular distance $|\Delta\eta_{JJ}| < 1.7$. Following further requirements on the jet masses, a signal region is defined in the $(m_J^{\text{lead}}, m_J^{\text{sub-lead}})$ phase-space centered at (124 GeV; 115 GeV), corresponding to the reconstructed masses of the two (leading and sub-leading) $H \rightarrow bb$ candidates, each reconstructed as a single large- R jet. Similarly to the data-driven estimation method employed in the case of resolved topologies, multi-jet templates are built from "lower-tagged" event selections (i.e. in which one of the large- R jet has no b -tagged track-jet and at least one failing b -tagging) and the kinematic distributions of the non- b -tagged J is re-weighted in order to mimic a H candidate. The shape of the $t\bar{t}$ background is taken from simulation. Finally, the normalisation of the backgrounds is obtained from binned likelihood fits of the leading large- R jet mass distribution in a sideband region. After successful validation of the background model in a dedicated region between the sideband and signal regions of the $(m_J^{\text{lead}}, m_J^{\text{sub-lead}})$ phase-space, the m_{JJ} distribution in the signal region is used as a discriminant, after correction of the large- R jet momenta by m_H/m_J , separately for events with two, three and four b -tags, see Figure 4.

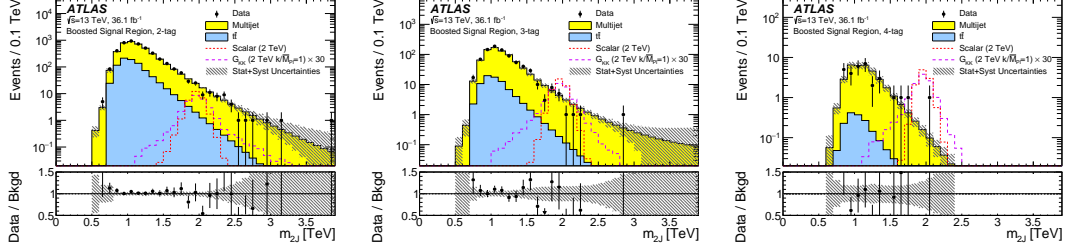


Figure 4: Reconstructed invariant mass of the two $H \rightarrow bb$ candidates in the signal region of the boosted topology, split by number of b -tags [17].

2.3 Results

The 95% confidence-level (CL) exclusion limits on the non-resonant HH production are shown in Table 1, in units of the SM prediction. In the case of $HH \rightarrow bbbb$ production through a spin-0 resonance, a statistical combination of the resolved and boosted topologies is performed in the mass range where they overlap, i.e. 800–1400 GeV. The 95% CL upper limits on the resonant production cross-section are shown in Figure 5.

Table 1: 95% CL limits on non-resonant Higgs boson pair production, from the search for $HH \rightarrow bbbb$ in ATLAS.

Observed	-2σ	-1σ	Expected	$+1\sigma$	$+2\sigma$
13.0	11.1	14.9	20.7	30.0	43.5

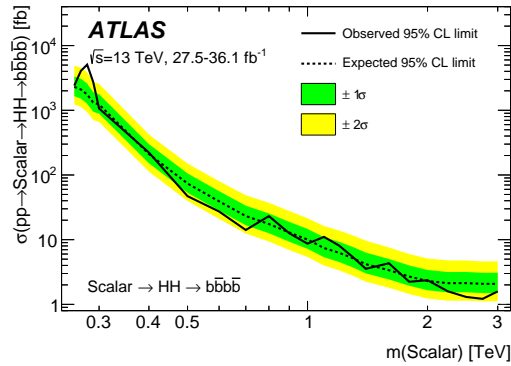


Figure 5: 95% CL limits on Higgs boson pair production from a spin-0 resonance, as a function of the hypothesised mass, from the search for $HH \rightarrow bbbb$ in ATLAS [17].

3 Search for $HH \rightarrow bb\gamma\gamma$ in ATLAS

The search for $HH \rightarrow bb\gamma\gamma$ suffers from a low signal branching fraction (0.26%), but the presence of a di-photon system with a good mass resolution provides a very clean signature. The event selection starts with a di-photon trigger, with transverse energy (E_T) thresholds at 25 and 35 GeV. Two photons with an invariant mass $m_{\gamma\gamma}$ between 105 and 160 GeV are selected, with $E_T/m_{\gamma\gamma}$ above 0.35 (0.25) for the leading (sub-leading) photon. The event selection proceeds with requesting at least two central jets with $p_T > 25$ GeV, vetoing events with more than two b -tags. The signal region consists of events with exactly two b -tags (with the same working point as in the search for $HH \rightarrow bbbb$.) and events with one b -tag, however with a tighter working point corresponding to a 60% efficiency. In that latter case, a Boosted Decision Tree (BDT) is used to assign a second jet to the $H \rightarrow bb$ candidate. In addition to the requirements on the photons and b -jets, two sets of event selections are applied:

- loose selection, used in the search for non-resonant production with a Higgs self-coupling different from the SM prediction and in the search for a spin-0 resonance of mass 260–500 GeV decaying via $HH \rightarrow bb\gamma\gamma$: the p_T of the leading (sub-leading) jet is greater than 40 (25) GeV, the invariant mass of the two jets is $80 \text{ GeV} < m_{jj} < 140 \text{ GeV}$ and, in the case of the search for resonant $HH \rightarrow bb\gamma\gamma$ production, $m_{\gamma\gamma}$ must be within 4.7 GeV of m_H ;
- tight selection, used in the search for SM non-resonant production and in the search for a spin-0 resonance heavier than 500 GeV decaying via $HH \rightarrow bb\gamma\gamma$: the p_T of the leading (sub-leading) jet is greater than 100 (30) GeV, the invariant mass of the two jets is $90 \text{ GeV} < m_{jj} < 140 \text{ GeV}$ and, in the case of the search for resonant $HH \rightarrow bb\gamma\gamma$ production, $m_{\gamma\gamma}$ must be within 4.3 GeV of m_H .

3.1 Search for non-resonant $HH \rightarrow bb\gamma\gamma$ production

The analysis strategy used in the search for non-resonant $HH \rightarrow bb\gamma\gamma$ production is to extract the signal from the $m_{\gamma\gamma}$ distribution. Both the HH signal and the single- H backgrounds are taken from simulation, and $m_{\gamma\gamma}$ is parameterised with a double-sided Crystal-Ball function. On the other hand, the continuum background of multi-jet and multi-photon events is modelled by a fit to the data, with a first-order exponential function. This fit function was found to minimise the spurious signal, i.e. the bias measured by fitting a signal+background model to a background-only sample. Figure 6 shows the $m_{\gamma\gamma}$ distribution in the signal region with one and two b -tags, obtained with the tight selection. In the absence of a statistically significant excess with respect to the SM prediction, 95% CL exclusion limits are set of the Higgs boson pair production cross-section, in units of the SM prediction, see Table 2.

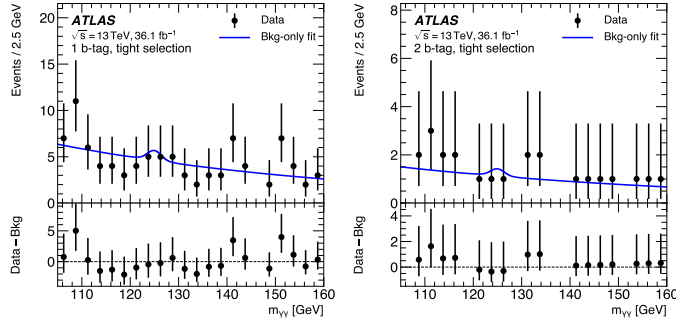


Figure 6: Di-photon mass spectrum in signal regions of the search for $HH \rightarrow bb\gamma\gamma$ in ATLAS, with one (left) or two (right) b -tags, after applying a tight event selection [18].

Table 2: 95% CL limits on non-resonant Higgs boson pair production, from the search for $HH \rightarrow bb\gamma\gamma$ in ATLAS.

Observed	-1σ	Expected	$+1\sigma$
22	20	28	40

Higgs self-coupling values that differ from the SM prediction affect the signal acceptance. The variations of the exclusion limits with κ_λ , defined as the ratio of the Higgs self-coupling λ to its predicted value in the SM, λ_{SM} , are computed with the loose event selection and are shown in Figure 7. As a result, κ_λ is constrained at the 95% CL to be between -8.2 and 13.2 .

3.2 Search for resonant $HH \rightarrow bb\gamma\gamma$ production

The analysis strategy used in the search for resonant $HH \rightarrow bb\gamma\gamma$ production is to extract the signal from the $m_{\gamma\gamma jj}$ distribution, after scaling the di-jet four-momentum by m_H/m_{jj} . The resonant HH signal is modelled with a Gaussian distribution with exponential tails. The single- H and SM non-resonant HH backgrounds are taken from simulation. On the other hand, the continuum background of multi-jet and multi-photon events is modelled by a fit to the data, with a fit function chosen to minimise the spurious signal. Figure 8 shows the $m_{\gamma\gamma jj}$ distribution in the signal region with one and two b -tags, obtained with the loose selection. In the absence of a statistically significant excess with respect to the SM prediction, 95% CL exclusion limits are set of the resonant Higgs boson pair production cross-section, see Figure 9.

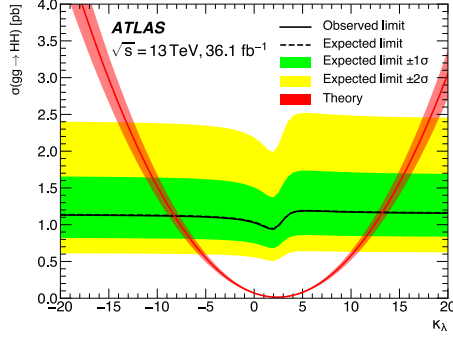


Figure 7: 95% CL limits on non-resonant Higgs boson pair production as a function of κ_λ , from the search for $HH \rightarrow bb\gamma\gamma$ in ATLAS. The red line indicates the theoretical prediction with its uncertainty [18].

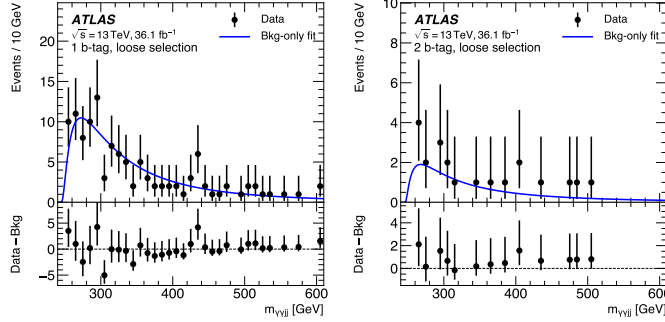


Figure 8: Distribution of $m_{\gamma\gamma jj}$ in signal regions of the search for $HH \rightarrow bb\gamma\gamma$ in ATLAS, with one (left) or two (right) b -tags, after applying a loose event selection [18].

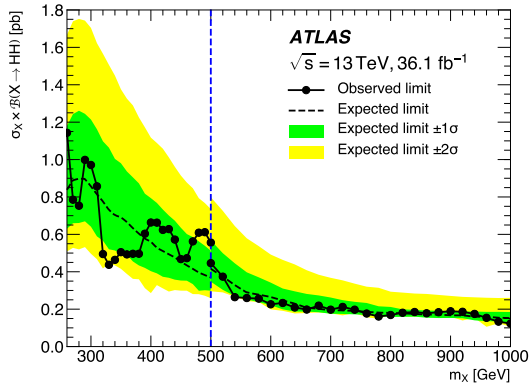


Figure 9: 95% CL limits on Higgs boson pair production from a spin-0 resonance, as a function of the hypothesised mass, from the search for $HH \rightarrow bb\gamma\gamma$ in ATLAS. The vertical blue dashed line indicates a change in event selections [18].

4 Search for $HH \rightarrow WW\gamma\gamma$ in ATLAS

The good mass resolution of the di-photon system arising from a $H \rightarrow \gamma\gamma$ decay has also been exploited to search for $HH \rightarrow WW\gamma\gamma$ in ATLAS, where one W -boson decays hadronically and the other one into a charged lepton (electron or muon) and a neutrino. The trigger, as well as the selection and reconstruction of the two photons coming from the $H \rightarrow \gamma\gamma$ decay are similar to those employed in the $HH \rightarrow bb\gamma\gamma$ search, except that $m_{\gamma\gamma}$ is required to be within 3.4 GeV of m_H when searching for both non-resonant and resonant Higgs boson pair productions. In addition, a requirement $p_T^{\gamma\gamma} > 100$ GeV is used in the search for SM non-resonant production and in the search for a spin-0 resonance heavier than 400 GeV. In order to select $H \rightarrow WW$ decays, events are also requested to have at least one electron or muon with $p_T > 10$ GeV, and at least two central jets which are not b -tagged. Both the HH signal and the single- H backgrounds are taken from simulation, and their $m_{\gamma\gamma}$ spectrum is parameterised with a double-sided Crystal-Ball function. On the other hand, the continuum background of multi-jet and multi-photon events is modelled by a fit to the data, with a second-order exponential function, chosen to minimise the spurious signal.

Figure 10 shows the predicted and measured $m_{\gamma\gamma}$ distribution when using or not the cut $p_T^{\gamma\gamma} > 100$ GeV. In the absence of a statistically significant excess with respect to the SM prediction, 95% CL exclusion limits are set of the non-resonant Higgs boson pair production cross-section, in units of the SM prediction (see Table 3), and on the cross-section for a spin-0 resonance decaying to HH (see Figure 11).

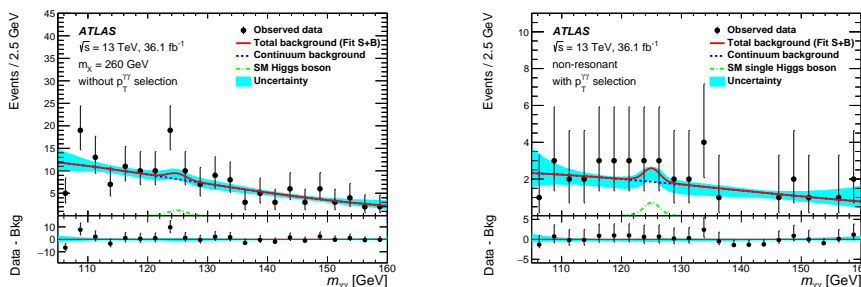


Figure 10: Di-photon mass spectrum in signal regions of the search for $HH \rightarrow WW\gamma\gamma$ in ATLAS, without (left) or with (right) a cut on $p_T^{\gamma\gamma}$ [19].

Table 3: 95% CL limits on non-resonant Higgs boson pair production, from the search for $HH \rightarrow WW\gamma\gamma$ in ATLAS.

Observed	-2σ	-1σ	Expected	$+1\sigma$	$+2\sigma$
230	90	120	160	240	340

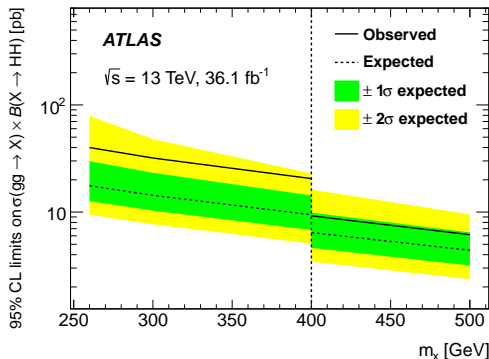


Figure 11: 95% CL limits on Higgs boson pair production from a spin-0 resonance, as a function of the hypothesized mass, from the search for $HH \rightarrow WW\gamma\gamma$ in ATLAS. The vertical dashed line indicates a change in event selections [19].

5 Conclusion

These proceedings report on three searches for Higgs boson pair production in up to 36.1 fb^{-1} of LHC pp collision data, which have been recently published by the ATLAS Collaboration: $HH \rightarrow bbbb$, $HH \rightarrow bb\gamma\gamma$ and $HH \rightarrow WW\gamma\gamma$. The data were analysed to search for non-resonant production of HH pairs as well as for heavy resonances decaying to two SM-like Higgs bosons, with various analysis strategies and event selections. The result of a fourth search, based on the $HH \rightarrow bb\tau\tau$ final state, was published after the conference [21], reaching 95% CL exclusion limits of 12.7 times the SM expectation for the non-resonant HH production mode. A statistical combination of the three most sensitive searches was also performed by ATLAS recently [22]. The combined observed limit on the non-resonant Higgs boson pair cross-section is 0.223 pb at 95% CL, which is equivalent to 6.7 times the predicted SM cross-section. The ratio κ_λ of the Higgs boson self-coupling to its SM expectation is constrained at 95% CL to $-5.0 < \kappa_\lambda < 12.1$. The search for Higgs boson pair production will remain at the core of the ATLAS research program towards the end of the LHC Run-2 and beyond, as it allows to probe directly the Higgs potential as well as search for new physics in the Higgs sector.

Copyright [2018] CERN for the benefit of the ATLAS Collaboration. Reproduction of this article or parts of it is allowed as specified in the CC-BY-4.0 license.

References

- [1] ATLAS Collaboration, *Observation of a new particle in the search for the Standard Model Higgs boson with the ATLAS detector at the LHC*, Phys. Lett. B **716** (2012) 1, arXiv: 1207.7214 [hep-ex].
- [2] CMS Collaboration, *Observation of a new boson at a mass of 125 GeV with the CMS experiment at the LHC*, Phys. Lett. B **716** (2012) 30, arXiv: 1207.7235 [hep-ex].
- [3] F. Englert and R. Brout, *Broken Symmetry and the Mass of Gauge Vector Mesons*, Phys. Rev. Lett. **13** (1964) 321.
- [4] P. W. Higgs, *Broken Symmetries and the Masses of Gauge Bosons*, Phys. Rev. Lett. **13** (1964) 508.
- [5] ATLAS and CMS Collaborations, *Combined Measurement of the Higgs Boson Mass in pp Collisions at $\sqrt{s} = 7$ and 8 TeV with the ATLAS and CMS Experiments*, Phys. Rev. Lett. **114** (2015) 191803, arXiv: 1503.07589 [hep-ex].
- [6] ATLAS and CMS Collaborations, *Measurements of the Higgs boson production and decay rates and constraints on its couplings from a combined ATLAS and CMS analysis of the LHC pp collision data at $\sqrt{s} = 7$ and 8 TeV*, JHEP **08** (2016) 045, arXiv: 1606.02266 [hep-ex].
- [7] D. de Florian et al. (LHC Higgs Cross Section Working Group), *Handbook of LHC Higgs Cross Sections: 4. Deciphering the Nature of the Higgs Sector*, arXiv: 1610.07922 [hep-ph].
- [8] M. Grazzini et al., *Higgs boson pair production at NNLO with top quark mass effects*, JHEP **05** (2018) 059, arXiv: 1803.02463 [hep-ph].
- [9] A. Djouadi, *The anatomy of electroweak symmetry breaking Tome II: The Higgs bosons in the Minimal Supersymmetric Model*, Phys. Rept. **459** (2008) 1, arXiv: hep-ph/0503173 [hep-ph].
- [10] G. C. Branco et al., *Theory and phenomenology of two-Higgs-doublet models*, Phys. Rept. **516** (2012) 1, arXiv: 1106.0034 [hep-ph].
- [11] L. Randall and R. Sundrum, *A Large mass hierarchy from a small extra dimension*, Phys. Rev. Lett. **83** (1999) 3370, arXiv: hep-ph/9905221 [hep-ph].

- [12] ATLAS Collaboration, *The ATLAS Experiment at the CERN Large Hadron Collider*, JINST **3** (2008) S08003.
- [13] ATLAS Collaboration, *ATLAS Insertable B-Layer Technical Design Report*, ATLAS-TDR-19, <https://cds.cern.ch/record/1291633>.
- [14] ATLAS Collaboration, *ATLAS Insertable B-Layer Technical Design Report Addendum*, ATLAS-TDR-19-ADD-1, <https://cds.cern.ch/record/1451888>.
- [15] ATLAS Collaboration, *Performance of the ATLAS trigger system in 2015*, Eur. Phys. J. C **77** (2017) 317, arXiv: 1611.09661 [hep-ex].
- [16] ATLAS Collaboration, *Trigger Menu in 2016*, ATL-DAQ-PUB-2017-001, <https://cds.cern.ch/record/2242069>.
- [17] ATLAS Collaboration, *Search for pair production of Higgs bosons in the $b\bar{b}b\bar{b}$ final state using proton-proton collisions at $\sqrt{s} = 13$ TeV with the ATLAS detector*, arXiv: 1804.06174 [hep-ex].
- [18] ATLAS Collaboration, *Search for Higgs boson pair production in the $\gamma\gamma b\bar{b}$ final state with 13 TeV pp collision data collected by the ATLAS experiment*, arXiv: 1807.04873 [hep-ex].
- [19] ATLAS Collaboration, *Search for Higgs boson pair production in the $\gamma\gamma WW^*$ channel using pp collision data recorded at $\sqrt{s} = 13$ TeV with the ATLAS detector*, arXiv: 1807.08567 [hep-ex].
- [20] M. Cacciari, G. P. Salam and G. Soyez, *The anti-kt jet clustering algorithm*, JHEP **04** (2008) 063, arXiv: 0802.1189 [hep-ph].
- [21] ATLAS Collaboration, *A search for resonant and non-resonant Higgs boson pair production in the $b\bar{b}\tau^+\tau^-$ decay channel in pp collisions at $\sqrt{s} = 13$ TeV with the ATLAS detector*, arXiv: 1808.00336 [hep-ex].
- [22] ATLAS Collaboration, *Combination of searches for Higgs boson pairs in pp collisions at 13 TeV with the ATLAS experiment*, ATLAS-CONF-2018-043.